

ARMA 22-0449



Permeability changes of damaged rock salt adjacent to inclusions of different stiffness

Ishtiaque Anwar and John C. Stormont

University of New Mexico, Albuquerque, NM, United States

Melissa M. Mills and Edward N. Matteo

Sandia National Laboratories, Albuquerque, NM, United States

Copyright 2022 ARMA, American Rock Mechanics Association

This paper was prepared for presentation at the 56th US Rock Mechanics/Geomechanics Symposium held in Santa Fe, New Mexico, USA, 26-29 June 2022. This paper was selected for presentation at the symposium by an ARMA Technical Program Committee based on a technical and critical review of the paper by a minimum of two technical reviewers. The material, as presented, does not necessarily reflect any position of ARMA, its officers, or members. Electronic reproduction, distribution, or storage of any part of this paper for commercial purposes without the written consent of ARMA is prohibited. Permission to reproduce in print is restricted to an abstract of not more than 200 words; illustrations may not be copied. The abstract must contain conspicuous acknowledgement of where and by whom the paper was presented.

ABSTRACT: Rock salt is being considered as a medium for energy storage and radioactive waste disposal. A Disturbed Rock Zone (DRZ) develops in the immediate vicinity of excavations in rock salt, with an increase in permeability, which alters the migration of gases and liquids around the excavation. When creep occurs adjacent to a stiff inclusion such as a concrete plug, it is expected that the stress state near the inclusion will become more hydrostatic and less deviatoric, promoting healing (permeability reduction) of the DRZ. In this scoping study, we measured the permeability of DRZ rock salt with time adjacent to inclusions (plugs) of varying stiffness to determine how the healing of rock salt, as reflected in the permeability changes, is a function of the stress and time. Samples were created with three different inclusion materials in a central hole along the axis of a salt core: (i) very soft silicone sealant, (ii) sorel cement, and (iii) carbon steel. The measured permeabilities are corrected for the gas slippage effect. We observed that the permeability change is a function of the inclusion material. The stiffer the inclusion, the more rapidly the permeability reduces with time.

1. INTRODUCTION

Rock salt is being considered as a medium for energy storage and radioactive waste disposal (Schulze, Popp, & Kern, 2001; Tsang, Bernier, & Davies, 2005; Yang, Daemen, & Yin, 1999) due to its extremely low permeability and low porosity. During the construction and/or facility operations, a Disturbed Rock Zone (DRZ) or Excavation Damaged Zone (EDZ) develops in the immediate vicinity of the excavation, with an increase in permeability (Gevantman & Lorenz, 1981; Schulze et al., 2001; Tsang et al., 2005). The increased permeability of the DRZ alters the migration of gases and liquids near the excavation.

Due to the deviatoric stress state that develops around excavations, rock salt creeps. When creep occurs adjacent to a stiff inclusion such as a concrete plug, it is expected that the stress state near the inclusion will become more hydrostatic and less deviatoric, promoting self-healing (Gevantman & Lorenz, 1981; Yang et al., 1999) of the DRZ, including permeability reduction. Healing adjacent to a concrete plug would limit bypass of the plug through the DRZ and thus be conducive to establishing a more effective seal system.

Healing of DRZ salt is believed to occur as grain boundaries, damaged from deviatoric stresses, are forced back together and reestablish very tight contact and low permeability. Healing is a function of stress, temperature, moisture conditions, time, and quantity of impurities (e.g., clay). Although numerous experiments have been conducted on the consolidation and resulting permeability decrease of granular salt, less is known about the healing of damaged rock salt.

The objective of this scoping study is to inform future systematic analysis and evaluate the healing of DRZ rock salt, as reflected in the permeability changes, as a function of stress, time, and the stiffness of a central inclusion.

2. MATERIALS AND METHODS

Cylindrical samples of rock salt (10.2 cm diameter, 10.3 cm long) from the DRZ surrounding excavations of the Waste Isolation Pilot Plant (WIPP) were used in this study (Figure 1). The samples ends were polished dry, and a 2.4 cm diameter central hole was carefully drilled along the axis of the core.

Specimens were created with three different inclusion materials, and were labeled S1, S2, and S3. The properties of the central inclusions used in this study are presented below:

Specimen S1: soft type S sealant inclusion (Shore A hardness of 15, ASTM C-920) with a modulus of elasticity less than 2 GPa

Specimen S2: Sorel cement inclusion (a magnesium-based cementitious material) with a modulus of elasticity ~29 GPa (measured using Tinius Olson Compression equipment)

Specimen S3: stiff carbon steel inclusion with a Young's modulus of 200 GPa (epoxy used as filler had modulus of elasticity of about 92-109 GPa)

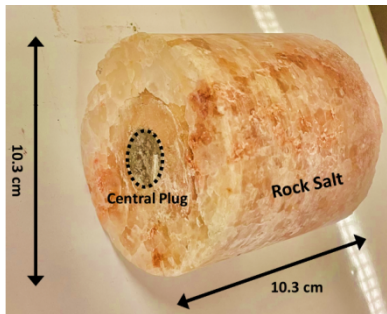


Figure 1 – Rock Salt specimen S3, with the central plug of carbon steel

A general overview of the experimental system is shown in Figure 2. The rock salt specimen is placed in a pressure vessel and subjected to hydrostatic stress conditions. Radial stress was applied to the specimen using hydraulic pressure behind a core holder sleeve that is integrated into the triaxial cell. The radial stress is always greater than the pore pressure to avoid fluid bypass along the sleeve-sample interface. An equivalent axial stress was applied to the specimen through the hydraulically activated end caps of the cell. The hydrostatic confining stress was monitored by a pressure gauge with an accuracy of 0.01 MPa. The hydrostatic stress during all tests reported here were conducted at 13.8 MPa, which corresponds to the expected geostatic stress at a depth of about 700 m.

A permeameter system was used to conduct steady-state gas permeability measurements. Gas injection line and pressure measurement transducers were connected to one of the end cap fittings. For all tests, the downstream line was vented to atmosphere. The upstream pressure was measured with pressure transducers (Omega DPG 409 and PX 409) with an accuracy of 1% of full scale. The gas flow rates were controlled using two mass flow controllers (Alicat Scientific Inc.) of different flow ranges (with accuracy $\pm 1\%$ of total flow range) connected in parallel to the upstream side of the specimen. Most of the flow test used the flow-controlled system for quickly achieving the steady-state. The pressure-controlled measurements were also used for measuring relatively

lower permeabilities ($< 10^{-21} \text{ m}^2$), and mass flow meter (Alicat Scientific Inc. with accuracy $\pm 2\%$ of total flow range) and soap bubble flow meter were collectively used to measure the flow rates. The nitrogen gas flow tests were conducted at $25 \pm 0.5^\circ \text{C}$. The typical test duration was 80 to 100 hours. During this time, the permeability as a function of time was observed.

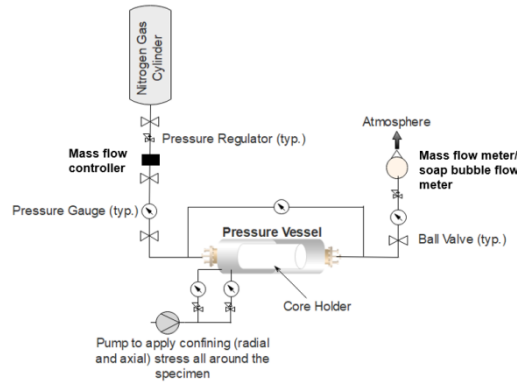


Figure 2 – Schematic of the flow test configuration

At sufficiently low flow rates, flow is described by Darcy's Law (Bear, 1972)

$$-\nabla P = \frac{\mu Q}{k A} \quad (1)$$

where ∇P is the pressure gradient, μ is the dynamic fluid viscosity, Q is the volumetric flow rate, k is the permeability, and A is the flow cross-sectional area.

For the steady-state flow of a real gas, Equation 1 can be rewritten as below for interpreting the permeability ((Anwar, Chojnicki, Bettin, Taha, & Stormont, 2019)

$$\frac{M(P_1^2 - P_2^2)}{2\rho z R \tau L} = \frac{\mu Q}{k A} \quad (2)$$

where M is the molecular weight, P_1 is the downstream pressure, P_2 is the upstream pressure, ρ is the gas density (based on the laboratory atmospheric pressure), z is the compressibility factor, R is the gas constant, τ is absolute temperature, L is the length over which pressure drop takes place.

Gas flow can be affected by molecular slip phenomenon, which arises due to the interaction between gas molecules and pore walls (Klinkenberg, 1941). The measured or apparent permeability (e.g., the permeability interpreted from Equation 1 or 2) can be related to the intrinsic or slip-corrected permeability (k_∞) as a linear function of reciprocal mean pressure (P_m) (Anwar et. al, 2019)

$$k = k_\infty \left(1 + \frac{b}{P_m} \right) \quad (3)$$

Commented [DT1]: Capitalize the "L"?

where b is the gas slippage factor. From the uncertainties in measured quantities, the error in the reported permeabilities is $\pm 5\%$ for each series of measurements.

3. RESULTS AND DISCUSSION

3.1. Flow test

Permeability and gas slippage factors of specimens S1, S2, and S3 were interpreted from measured gas flow data as described in the previous section. The permeability of the inclusion materials is required to interpret permeability from measured values. The permeability of the silicon and carbon steel was below the measuring capability of the laboratory permeameter and was considered impermeable. The permeability of a control specimen or blank prepared from sorel cement was measured. The permeability is about $2.8 \times 10^{-21} \text{ m}^2$, which is orders of magnitude lower than DRZ rock salt specimens at the same confining pressure.

The measured slip corrected permeabilities for all three different rock salt specimens and the sorel cement over time are graphically presented in Figure 3. The flow test results reveal that the initial DRZ rock salt permeabilities of all three specimens were in the range 10^{-14} to 10^{-15} m^2 . These values are orders of magnitude greater than that of intact rock salt which has an extremely low permeability (less than 10^{-20} m^2 (Sutherland & Cave, 1980)).

The rate of permeability reduction was different for the three specimens. The initial permeability of specimen S1, the DRZ rock salt specimen with the soft silicon plug under confining stress, was about $2 \times 10^{-15} \text{ m}^2$. The final permeability of the specimen, after 100 hours, was found to be about $9 \times 10^{-16} \text{ m}^2$.

For specimen S2, the DRZ rock salt specimen with the sorel cement, the initial permeability was about $1.5 \times 10^{-14} \text{ m}^2$, and the final permeability reduced to about $3.7 \times 10^{-21} \text{ m}^2$ after 80 hours. The permeability measured for specimen S3, the DRZ rock salt specimen with the steel rod, was initially about $3.5 \times 10^{-15} \text{ m}^2$ and the final permeability was found to be about $3 \times 10^{-21} \text{ m}^2$ after only 44 hours.

The slowest permeability reduction was observed for specimen S1 and the fastest permeability reduction was observed for specimen S3. As observed in Figure 3, the rate of permeability reduction for S2 was greater relative to the rate of permeability reduction for S1, but lower than the same of S3. The flow test measurement was terminated once the permeability of both the specimens S2 and S3 approached the permeability of the sorel cement.

3.2. Gas slippage factor

Gas slip factors as a function of measured permeability of rock salt are presented in Figure 4. The best-fit straight line through the data yields,

$$b = 1.47 k^{-0.31} \quad (4)$$

where the units of b and k are in Pa and m^2 , respectively.

Empirical relationships between gas slip factor and permeability derived from two previous studies (Heid, McMahon, Nielsen, & Yuster, 1950; Jones & Owens, 1980) are given in Table 1 for comparison to the present study. All three studies yield comparable relationships. The theoretical value of the exponent is -0.5 for an assumed geometry of uniform cylindrical capillaries; empirical exponent values less than -0.5 have been attributed to actual pore geometries differing from uniform cylindrical capillaries (Heid et al., 1950).

Commented [DT2]: May want to include reference and make this statement about "intact WIPP rock salt"???

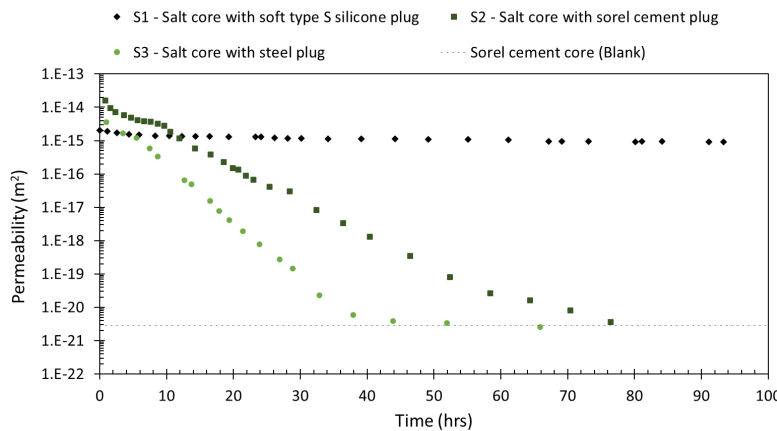


Figure 3 – Permeability of rock salt specimens adjacent to inclusions (plugs) of varying stiffness/ blank sorel cement, with time subjected to a hydrostatic or confining stress of 2000 psi (13.8 MPa)

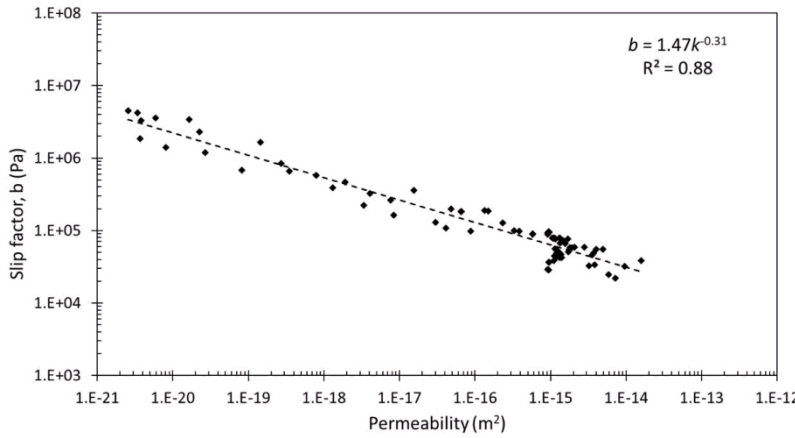


Figure 4: Equation correlating the gas slip factor and the permeability.

Table 1 Empirical equations for estimating gas slip factor (b) for different porous media

Correlations	Equation	permeability range (m^2)	Material (porous)
Heid et al. (Heid et al., 1950)	$b = 0.11 k^{-0.39}$	10^{-12} to 10^{-17}	Sandstone core
Jones and Owens (Jones & Owens, 1980)	$b = 0.98 k^{-0.33}$	10^{-14} to 10^{-19}	Low permeability sands
Current study	$b = 1.47 k^{-0.31}$	10^{-14} to 10^{-21}	Rock salt during healing

Note: The units of b and k are in Pa and m^2 , respectively.

4. CONCLUSION

The permeability of rock salt was interpreted from a series of gas flow measurements made under a hydrostatic stress with time.

These measurements reveal that rock salt from the DRZ has permeability orders of magnitude greater than intact rock salt. The permeability of specimen S1 (negligible stiffness, equivalent to no plug) did not decrease significantly with time, whereas the permeability of specimens S2 and S3 decreased orders of magnitude, to values similar to intact rock salt. The rate of permeability reduction was considerably greater for the specimen S3 (greatest stiffness). Hence, we conclude that the stiffer (greater modulus of elasticity) the central inclusion/ plug, the more rapidly the permeability of DRZ rock salt reduces with time.

The measurements included significant gas slippage. Consequently, gas slippage factors were determined for the specimens under confining stress and used in interpreting intrinsic permeability values from the data. An empirical relationship was found between the gas slip factor and permeability that is similar to relationships for other porous media.

The permeability measurements for different hydrostatic stresses were not included in the experimental study. To obtain a systematic relationship and to better understand the phenomenon, further analytical measurements such as volume strain measurement, structural integrity, porosity, damage measurement (via density or wave velocity measurement) and flow tests with multiple confining stresses is recommended for future studies.

ACKNOWLEDGEMENT

Sandia National Laboratories is a multi-mission laboratory managed and operated by National Technology and Engineering Solutions of Sandia, LLC., a wholly owned subsidiary of Honeywell International, Inc., for the U.S. Department of Energy's National Nuclear Security Administration under contract DE-NA0003525. This research is funded by WIPP programs administered by the Office of Environmental Management (EM) of the U.S. Department of Energy. SAND2022-XXXXX.

REFERENCES

1. Anwar, I., Chojnicki, K., Bettin, G., Taha, M. R., & Stormont, J. C. (2019). Characterization of wellbore casing corrosion product as a

permeable porous medium. *Journal of Petroleum Science and Engineering*, 180, 982–993.

- 2. Bear, J. (1972). Dynamics of flow in porous media. In *American Elsevier* (p. 764).
- 3. Gevantman, L. H., & Lorenz, J. (1981). *Physical properties data for rock salt* (Vol. 167). US Department of Commerce, National Bureau of Standards.
- 4. Heid, J. G., McMahon, J. J., Nielsen, R. F., & Yuster, S. T. (1950). Study of the permeability of rocks to homogeneous fluids. *Drilling and Production Practice*. American Petroleum Institute.
- 5. Jones, F. O., & Owens, W. W. (1980). A laboratory study of low-permeability gas sands. *Journal of Petroleum Technology*, 32(09), 1–631.
- 6. Klinkenberg, L. J. (1941). The permeability of porous media to liquids and gases. *Drilling and Production Practice*. American Petroleum Institute.
- 7. Schulze, O., Popp, T., & Kern, H. (2001). Development of damage and permeability in deforming rock salt. *Engineering Geology*, 61(2–3), 163–180.
- 8. Sutherland, H. J., & Cave, S. P. (1980). Argon gas permeability of New Mexico rock salt under hydrostatic compression. *International Journal of Rock Mechanics and Mining Sciences*, 17, 281–288.
- 9. Tsang, C.-F., Bernier, F., & Davies, C. (2005). Geohydromechanical processes in the Excavation Damaged Zone in crystalline rock, rock salt, and indurated and plastic clays—in the context of radioactive waste disposal. *International Journal of Rock Mechanics and Mining Sciences*, 42(1), 109–125.
- 10. Yang, C., Daemen, J. J. K., & Yin, J.-H. (1999). Experimental investigation of creep behavior of salt rock. *International Journal of Rock Mechanics and Mining Sciences*, 36(2), 233–242.